MICRO-OPTO-MECHANICAL PRESSURE SENSOR (MOMPS) IN SIN INTEGRATED PHOTONICS PLATFORM

R. Jansen*, V. Rochus*, J. Goyvaerts**, G. Vandenboch**, B. van de Voort***, P. Neutens*, J. O' Callaghan*, H.A.C. Tilmans*, and X. Rottenberg*

*IMEC, Kapeldreef 75, Leuven 3001, Belgium, jansenr@imec.be
**KU Leuven, Leuven 3000, Belgium
*** Masdar institute, UAE

ABSTRACT

This paper presents a Micro-Opto-Mechanical Pressure Sensor (MOMPS) manufactured in a SiN integrated photonic platform in the near-IR (NIR). It is implemented with a single wavelength Mach Zehnder Interferometer (MZI) system that relies on a single readout detector that could be integrated on CMOS.

We report a measured accuracy of 9 Pa at a 1.2 Hz sampling rate for a device with a range of 4kPa and 0.7mm membrane diameter, which is comparable to available piezo and capacitive pressure sensors. This performance, which to our knowledge is the first reported measured accuracy for MZI MOMPS, demonstrates the potential of MOMPS which can be further unlocked with planned improvements and optimization of design. In this work we detail the working of the MZI MOMPS, and describe the measurement techniques and results.

Keywords: MOMPS, MZI, SiN, pressure, sensor

1 INTRODUCTION

The ability to use integrated optics together with micromachined mechanical parts allows a wide range of possibilities. Small mechanical displacements can result in a large effect on the optical circuit. This is one of the reasons MOMPS are predicted to have improved sensitivity and noise performance compared to their piezoelectric and capacitive counterparts [1]. Furthermore, the sensitivity of modern detectors and imagers paired with the power levels from laser components result in high signal to low noise levels. Integration, especially for the laser component, however remains challenging.

MOMPS have been demonstrated using MZIs [2] or ring resonators [3,4]. These approaches typically measure a shift in the frequency response of the device, which means that either a tunable source or broadband source used with a spectrometer is needed to obtain a readout. Neither of these approaches lend themselves to integration on a single device with a small footprint. In this paper, we demonstrate a single wavelength system based on a SiN integrated photonic MZI in the near-IR (NIR), with a single readout detector. A low temperature PECVD SiN is used as waveguide core and manufactured with 200 mm DUV lithography [5], which means the MZI MOMPS can be post-processed directly on CMOS imager/detector wafers.

2 WORKING PRINCIPLE

The MOMPS reported combines the optical and mechanical design by integrating a MZI system on top of a pressure sensitive membrane.

MZIs split optical power into two propagation paths. The paths are then recombined, with the phase difference between them reported at the output. In this design the MZI is implemented with integrated single mode photonic waveguides, with multi-mode interferometers (MMIs) used to split and re-combine the light.

One of the MZI arms is placed on top of the membrane, which is displaced as a result of differential pressure applied to the device, while the other acts as a fixed reference. Figure 1 shows a layout of such a MZI device, demonstrating how a folded spiral is used to increase the optical path length on top of the membrane.

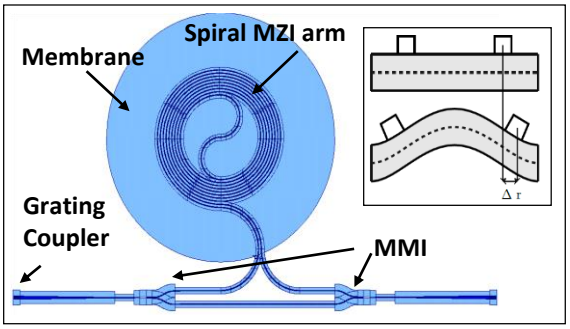

Figure 1: A layout of a Mach Zehnder Interferometer (MZI), shown with grating couplers, MMI splitters, and spiral waveguide arm over a membrane.

The membrane is created by using a backside etch to selectively remove parts of the silicon substrate underneath the optical stack. Figure 2 shows a cross section of the device, demonstrating how the SiN embedded between two oxide is released with the backside silicon etch.

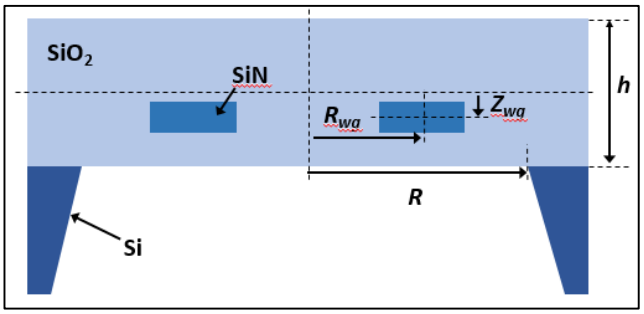

Figure 2: Cross-section of a MOMPS, showing the SiN waveguide layer, the oxide cladding and the silicon substrate. The geometrical parameters indicated are for a circular waveguide and its placement relative to the membrane and will be used in the analysis of the device.

3 THEORETICAL ANALYSIS

If we consider no losses, the output intensity coming from the MZI depends on the phase difference $\Delta\phi$ between the two arms:

$$I_{out} = I_{in}\cos(\frac{\Delta\phi}{2})^2 \quad (1)$$

The phase difference between the two MZI arms is computed by the following equation

$$\Delta\phi = \frac{2\pi}{\lambda_0} L_0 \Delta n_{eff} + \frac{2\pi}{\lambda_0} n_{eff} \Delta L + C \quad (2)$$

where λ_0 is the wavelength in vacuum, n_{eff} is the effective refractive index of the waveguide, Δn_{eff} the variation in effective refractive index (due to the elasto-optic effect and geometrical deformation), L_0 is the length of the sensing arm and ΔL is the length variation of the sensing arm. The last term C takes into account the fixed difference of length between the two arms, while the opto-mechanical coupling appears in the two first terms.

For the designs in this paper the length variation ΔL due to the bending of the membrane dominates the behavior [6], and we simplify (2) as:

$$\Delta\phi = \frac{2\pi}{\lambda_0} n_{eff} \Delta L \quad (3)$$

In the case of a circular membrane, the length variation of a ring waveguide is described by the equation

$$\Delta L = 2\pi \Delta r \quad (4)$$

where Δr is the waveguide radius variation due to the deformation.

The vertical displacement w of the ring waveguide on the membrane due to a pressure difference ΔP between the two sides is computed by the equation [7]

$$w = \frac{\Delta P}{64\, D + 4hR^2\sigma_0}(R^2 - {R_{wg}}^2)^2 \quad (5)$$

where R is the membrane radius, R_{wg} is the position of the ring waveguide (see Figure 2), σ_0 is the stress in the membrane, and

$$D(h) = \frac{E\, h^3}{12\,(1-\upsilon^2)} \quad (6)$$

where h is the thickness, E the Young modulus and ν the Poisson ratio. The radial displacement of the waveguide is derived by

$$u_r = -Z_{wg}\frac{\partial w}{\partial R_{wg}} = \frac{Z_{wg}\Delta P\, R_{wg}}{16\, D + hR^2\sigma_0}(R^2 - {R_{wg}}^2) \quad (7)$$

where Z_{wg} is the vertical position of the waveguide with referecne to the center of the membrane (see Figure 2) . We will now compute the effect of the variation of the waveguide length, ΔL. It can be computed using the lateral displacement ur by the relation:

$$\Delta L = 2\pi u_r \quad (8)$$

Using equations (7) and (8), we find:

$$\Delta\phi = \frac{2\pi}{\lambda_0} n_{eff} \frac{2\pi \Delta P Z_{wg} R_{wg}}{16D + hR^2\sigma_0}\left(R^2 - {R_{wg}}^2\right) \quad (9)$$

From equation (1), the output intensity will vary from 1 to 0 when the phase difference varies from 0 to π. So at $\Delta\phi = \pi$, we have covered the first pressure range. We can then define the full pressure range as

$$\Delta P_{range} = \frac{\lambda_0}{4\pi n_{eff}} \frac{16D + hR^2\sigma_0}{Z_{wg} R_{wg}(R^2 - {R_{wg}}^2)} \quad (10)$$

When the waveguide configuration has a spiral form, we can use the previous equations and replace the full pressure range by

$$\Delta P_{range} = \frac{\lambda_0}{4\pi n_{eff}} \frac{16D + hR^2\sigma_0}{Z_{wg} \sum_{i=1}^{N} R_{wg\,i}\,(R^2 - {R_{wg\,i}}^2)} \quad (11)$$

In this case the sensitivity is effectively multiplied by the number of loops (as long as the loops are in the sensitive part of the membrane). In Figure 3 the responses of two devices with 1 and 5 spiral waveguide loops respectively shown. The linear part of the response curve and the ΔP are indicated.

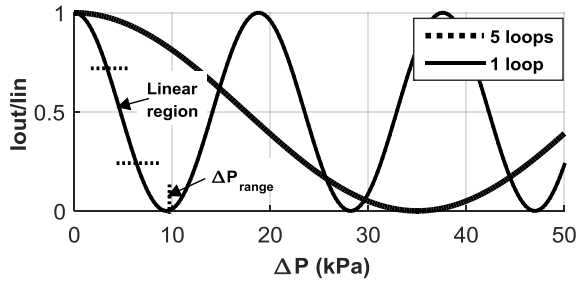

Figure 3: Relative output intensity versus applied pressure for a 500µm radius membrane, for a device with either 1 or 5 spiral waveguide loops.

4 MEASUREMENT SETUP

A schematic overview of the measurement system used to characterize the devices reported here is shown in Figure 4. The differential MOMPS are placed on a custom pressure chamber, in which the pressure is controlled with a commercial system, comprising of a controller, a pump,a reference sensor and a control valve, allowing PID control of the chamber pressure.

Optical power is coupled in and out of the circuit using optical fibers aligned to grating couplers, with a power meter used to measure the output power. The pressure and optical systems are controlled from a single PC.

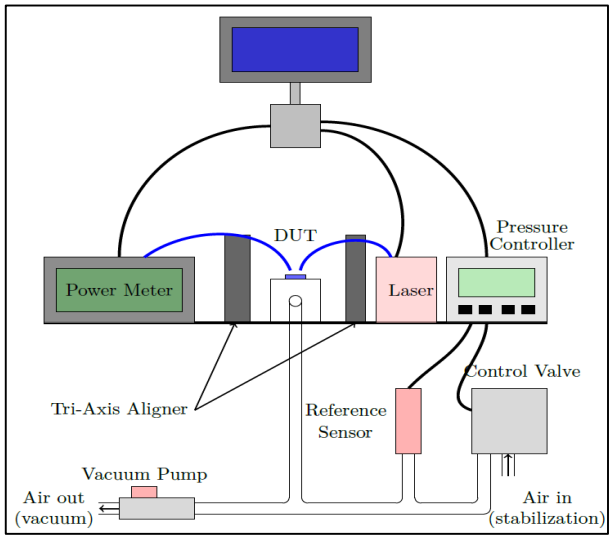

Figure 4: Schematic overview of the measurement setup.

5 MEASURED RESPONSE AND FITTING

The optical layers in this demonstrator had been optimized for optical performance only, and showed a compressive stress when released with backside etch. This can be corrected in the future by taking care to balance the stress of the various layers. Figures 5 show profilometer measurenents of two devices, with 4um and no oxide cladding respectively. Microscope iamges of the devices are shown in Figure 6. The 4um oxide device shows less buckling, as the oxide layers compensate somewhat for the stress from the SiN layer.

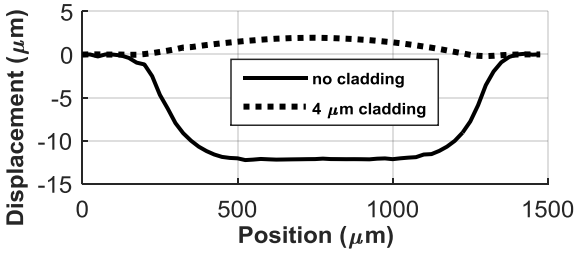

Figure 5: Profilometer measurements for two membranes, demonstrating that the devices are buckled due to compressive stress.

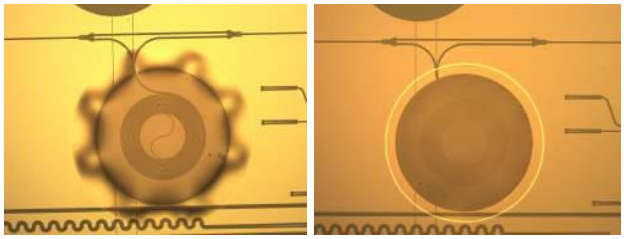

Figure 6: Microscope images of two membranes. The uncladded shows strong buckling and distortion in the surrounding.

In Figure 7 we present measured data from a MOMPS with a membrane radius of 250um, top cladding of 4um, and 9 spiral loops. The normalize data is fitted with a sine squared response as predicted from equations (1) and (11). The model lines up very well with measured values when using a compressive stress level of 45MPa. It should be said that the exact stress levels in the layer is not known, although 45MPa is in the predicted range (0-75MPA).

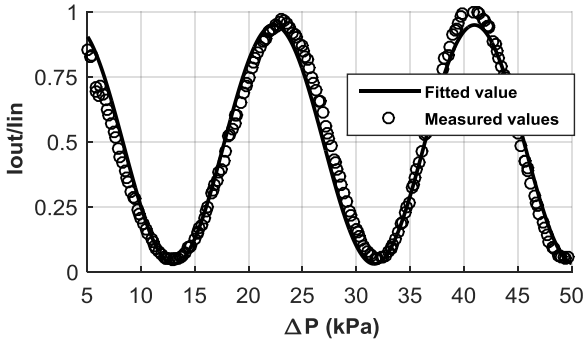

Figure 7: Measured normalized response value, showing a fitted value based on equation 11 and using a compressive stress value of 45MPa. Due to buckling (see Figures 5 and 6) of the device the behaviour around 0kPA was unreliable, so the fitting is done from 5kPa onwards.

6 RESOLUTION MEASUREMENT

The measurement setup described in the previoius section allows us to measure the sensitivity and range of the pressure sensor devices. However, the accuracy measurable by this system is limited by the accuracy and resolution of the reference sensor.

To overcome this limitation, a pressure release method with interpolation is used. A large differential pressure is applied after which the pump is switched off. The pressure in the chamber is allowed to slowly equalize to atmospheric pressure. During this equalization, a constant stream of laser power and pressure measurements are taken. The pressure leak is slow enough so that each for distinguishable drop in pressure difference measured from the reference pressures sensor, a large amount of optical power measurements are available. As a similar amount of optical points are also measured for each pressure point, we know the release in pressure is linear to the first order. This allows us to easily interpolate to find the expected pressure point for each detected optical power point.

By calculating the R squared fitting to a linear curve, and correlating the fitting error to a pressure value using the sensitivity of the device, we can reach a measured pressure accuracy.

Figure 8 gives the measured results for a device with membrane radius of 350um, along with a linear fitting, which when processed as described above results in a measured accuracy of 9 Pa at 1.2Hz sampling rate.

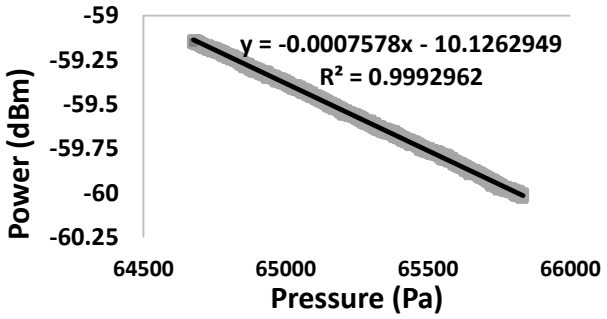

Figure 8: Data from a pressure release measurement, showing a linear fit on the interpolated values, which can be translated to an accuracy of 9 PA at 1.2Hz

7 DISCUSSION

This accuracy figure reported is limited by the noise factors of the measurement setup, such as the the laser amplitude and wavelength noise. Although the fibers were glued to the grating couplers to reduce vibrational noise, mechanical noise of the full setup was also a concern. Improvements in the measurement setup will decrease the effect of the mechacnicla noise in the lab, which will allow us to better meaure the he intrinsic capabilities of the sensor. The MZI devices presented in this work are unbalanced, which means that the reference arm has large difference in path length to the sensing arm. Although this is advantageous to reduce the footprint of the device, it leaves the sensor vulnerable to wavelength variations from the laser source. For future iterations we will compare the accuracy for balanced and unbalanced MZIs.

8 CONCLUSIONS

In this paper, we have demonstrated a MOMPS with a accuracy of 9 Pa at a 1.2Hz sampling rate for a device with a range of 4kPa and 0.7mm membrane diameter. This performance is comparable to existing capacitve and piezo pressure sensors, and shows the promise of our MOMPS as there is a view to a further reduction in the accuracy and also a expansion of range.

REFERENCES

[1] P. K. Pattnaik, A. Selvarajan, and T. Srinivas, “Guided wave optical mems pressure sensor. Sensors for Industry Conference”, Houston Texas, p. 122–125, 2005.

[2] H. Porte, V. Gorel, S. Kiryenko, G. Jean-Pierre, W. Daniau, and P. Blind, “Imbalanced mach-zehnder interferometer integrated in micromachined silicon substrate for pressure sensor” Journal of Lightwave Technology, 17(2):229–233, 1999.

[3] S.M.C. Abdulla, P.J. Harmsma, R.A. Nieuwland, and J. Pozo, “Soi based mechano-optical sensor using a folded micro-ring resonator”, 9th International Workshop on Nanomechanical Sensing (NMC 2012), *pp 80-81*.

[4] E. Hallynck and P. Bienstman. Integrated optical pressure sensors in silicon-on insulator, IEEE Photonics Journal, *4, Number 2, 2012*

[5] A.Z. Subramanian, P Neutens, A. Dakal, T. Claes, and R. Jansen, “Low-loss single mode pecvd silicon nitride photonic wire waveguides for 532-900 nm wavelength window fabricated within a cmos pilot line”, IEEE Photonics Journal 5(6), 2013

[6] V. Rochus, R. Jansen, J. Goyvaerts, G. Vandenboch, B. van de Voort, P. Neutens, J. O’ Callaghan, H.A.C. Tilmans, and X. Rottenberg, “Design of a MZI Micro-Opto-Mechanical Pressure Sensor for a SiN Photonics Paltform”, EuroSimE 2016

[7] S. Timoshenko and S. Woinowsky-Krieger. Theory of Plates and Shells. McGRAW-HILL, second edition edition, 1959.